

Coupling Nanowire Quantum Dots to Optical Waveguides by Microsphere Induced Photonic Nanojet

Symeon I. Tsintzos^{1,i}, Konstantinos Tsimvrakidis¹, James C. Gates², Ali W. Elshaari³, Peter G.R. Smith², Val Zwiller³, and Christos Riziotis^{*1,4}

¹Theoretical & Physical Chemistry Institute, National Hellenic Research Foundation, 11635 Athens, Greece

²Optoelectronics Research Centre, University of Southampton, SO17 1BJ Southampton, United Kingdom

³Department of Applied Physics, Royal Institute of Technology (KTH), 106 91 Stockholm, Sweden

⁴Institute for Advanced Modelling and Simulation, University of Nicosia, CY-2417 Nicosia, Cyprus

ⁱ Present address: QUBITECH Quantum Technologies, 15231 Chalandri, Athens, Greece

*Corresponding author (C. Riziotis): Tel: (+30) 2107273887, e-mail: Riziotis@eie.gr

Supplementary Material

The supplementary material provides details of the coupling mechanism, for the coupling arrangement configurations presented in section 3.2 of the manuscript, for microspheres of refractive indices with values $n = 1.6, 1.7, 1.76, 1.9, 2.0, 2.2,$ and $2.5,$ and with various diameters.

For each individual graph in Figure 4 of the manuscript corresponding to a specific refractive index, the following figures S1 - S7 present visually the coupling mechanism by the photonic nanojet's excitation, for various examined microspheres' diameters, and for a specific distance L which corresponds to the maximum observed coupling value. Each one of the Figures S1(a) -S7(a) presents the light propagation along $120\mu\text{m}$ distance, and also in Figures S1(b) -S7(b) a magnified version of the graphs of Figure 5, for a greater propagation distance of $70\mu\text{m}$. Figures S3(c), and S4(c) provide additionally, for comparison two indicative suboptimum coupling cases for comparison with the corresponding optimum cases.

It must be noted that in each Figure S1- S7 the scaling and color graphical color representation in the detailed propagation graph has been changed and enhanced to demonstrate the details of photonic nanojet generation and propagation and make visible microspheres' perimeter in relation to the nanojet formation.

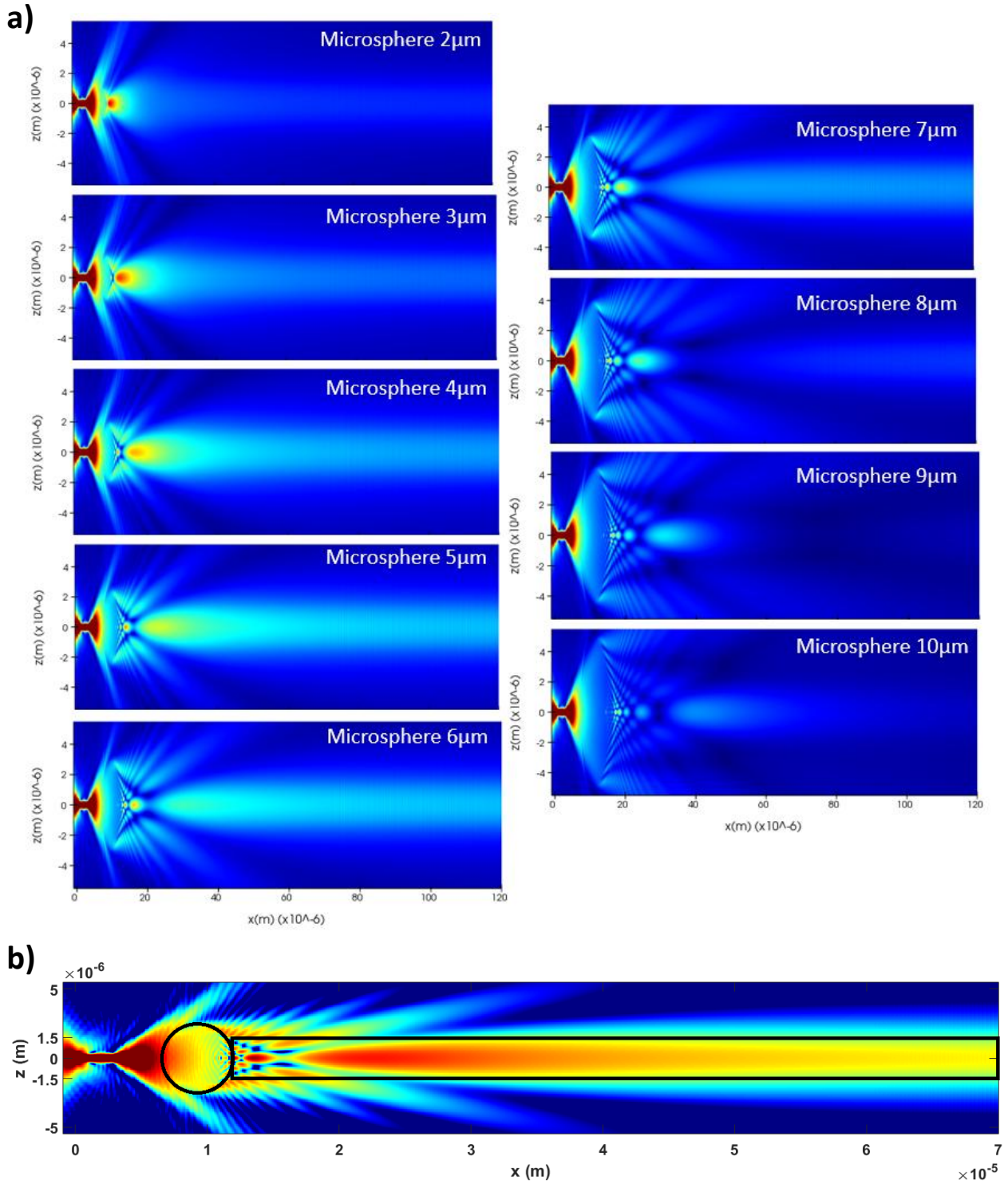


Figure S1. Coupling for a microsphere with $n=1.6$. a) Representative light propagation simulations, over 120 μm length, for specific diameters and distance $L=3\mu\text{m}$. b) Coupling mechanism for the optimum case with maximum coupling with diameter $5\mu\text{m}$ and $L=3\mu\text{m}$ over 70 μm propagation length.

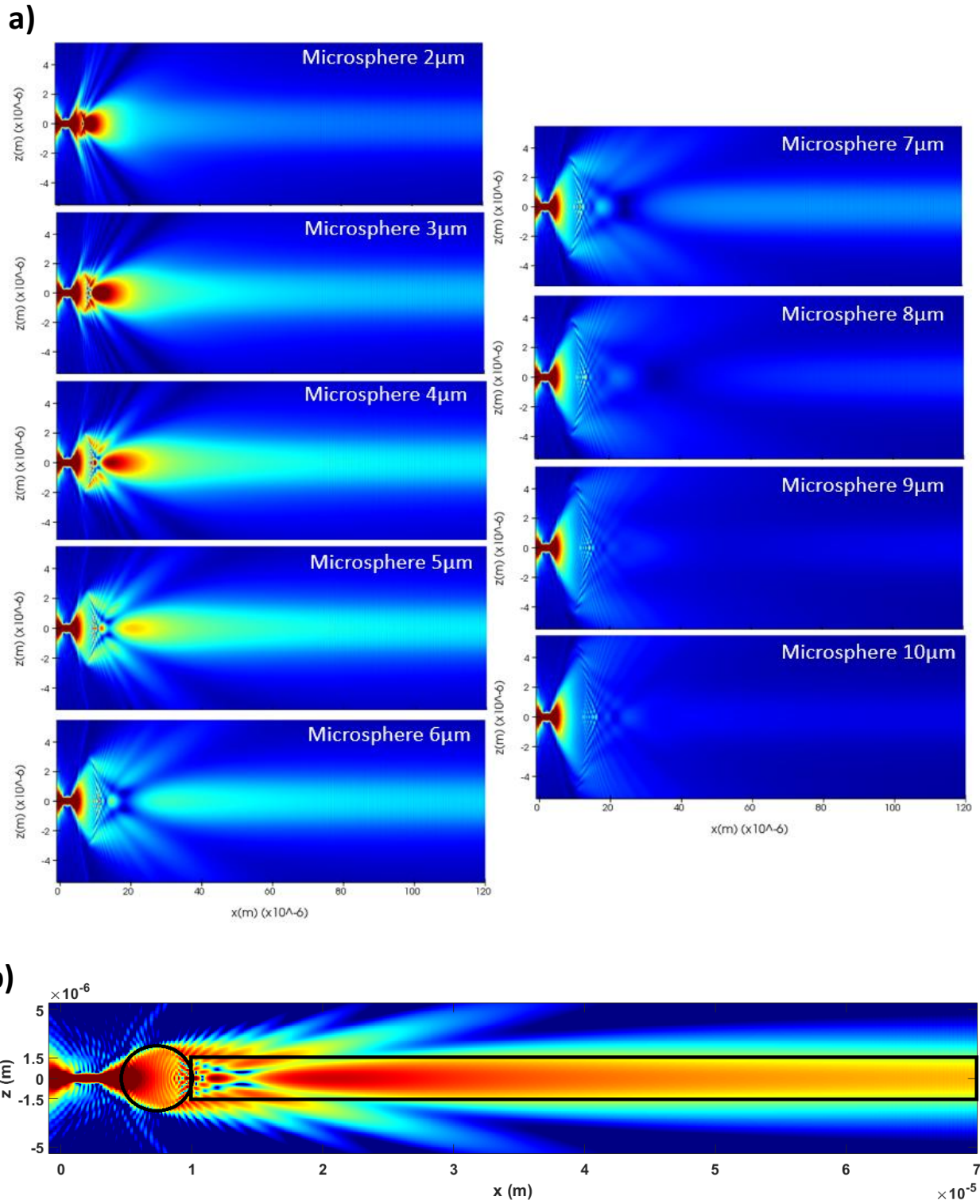


Figure S2. Coupling for a microsphere with $n=1.7$. a) Representative light propagation simulations, over $120\ \mu\text{m}$ length, for specific diameters and distance $L=1\ \mu\text{m}$. b) Coupling mechanism for the optimum case with maximum coupling with diameter $5\ \mu\text{m}$ and $L=1\ \mu\text{m}$ over $70\ \mu\text{m}$ propagation length.

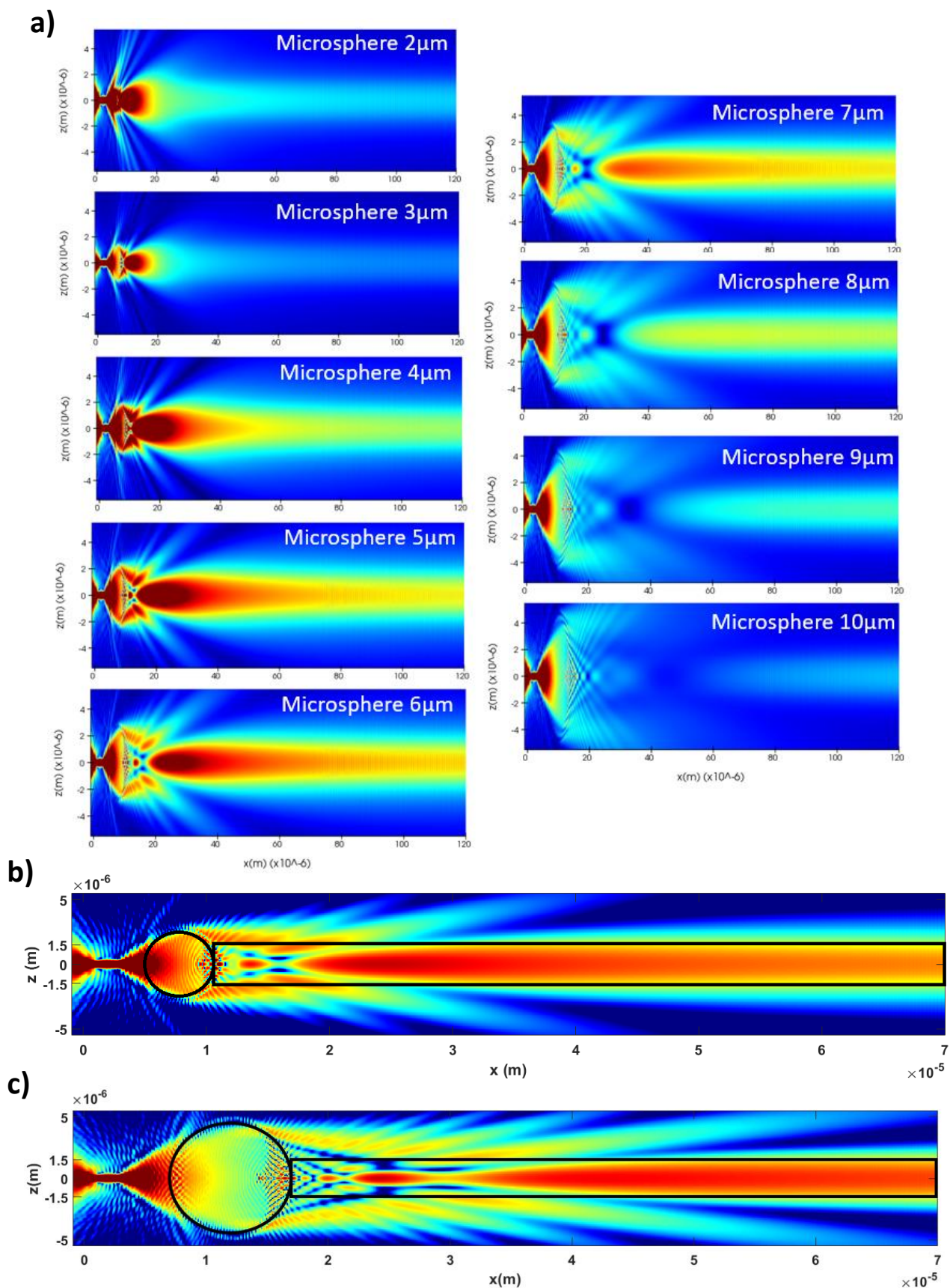


Figure S3. Coupling for a microsphere with $n=1.76$. a) Representative propagation simulations, over 120 μm length, for specific diameters and distance $L=1 \mu\text{m}$. b) Coupling mechanism for the optimum case with maximum coupling with diameter $6 \mu\text{m}$ and $L=1 \mu\text{m}$. c) Coupling mechanism for the suboptimum case with diameter $10 \mu\text{m}$ and $L=3 \mu\text{m}$, over 70 μm propagation length.

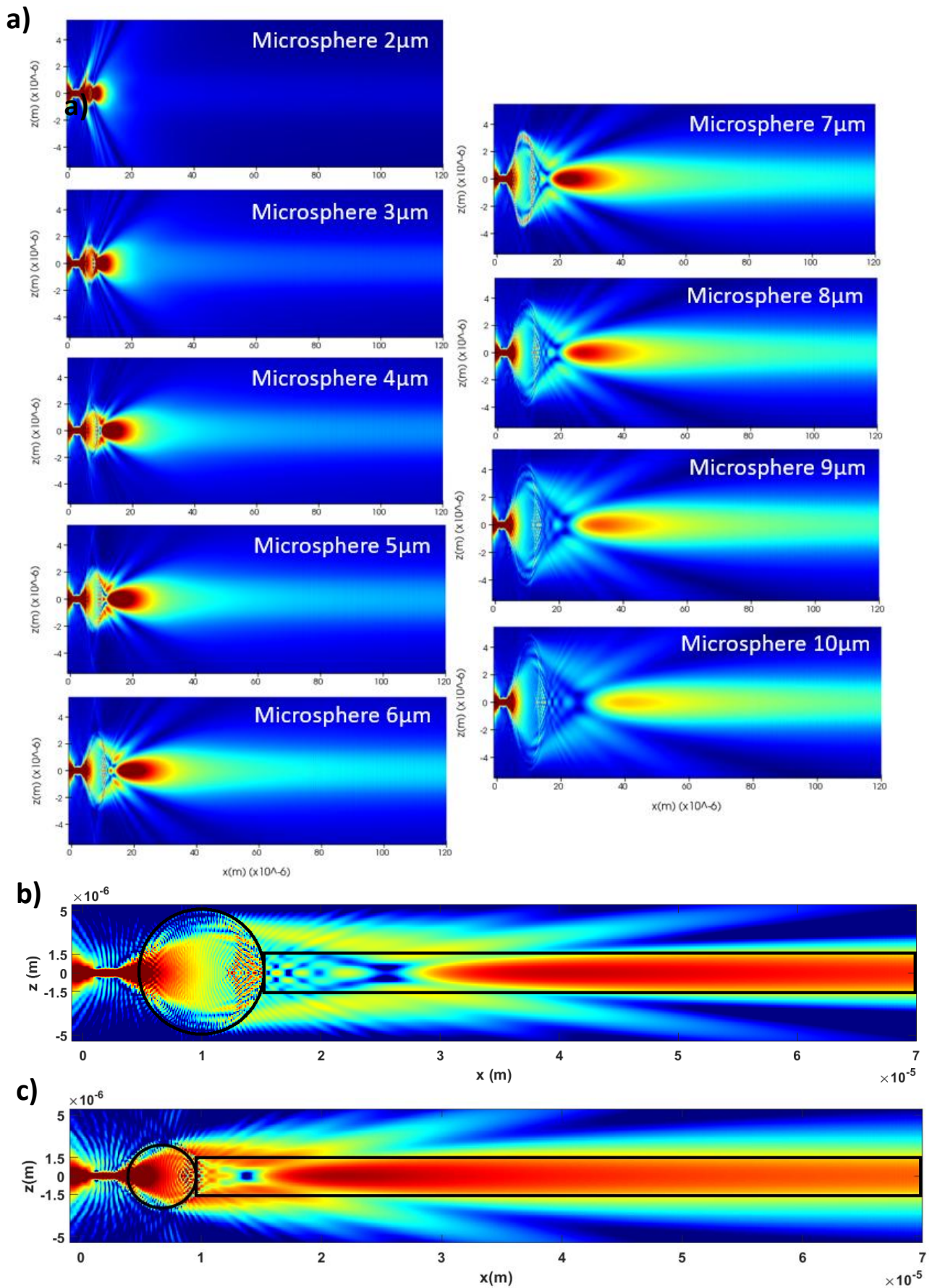


Figure S4. Coupling for a microsphere with $n=1.9$. a) Representative propagation simulations, over $120\ \mu\text{m}$ length, for specific diameters and distance $L=1\ \mu\text{m}$. b) Coupling mechanism for the optimum case with maximum coupling with diameter $10\ \mu\text{m}$ and $L=1\ \mu\text{m}$, c) Coupling for the suboptimum case with diameter $6\ \mu\text{m}$ and $L=0\ \mu\text{m}$, over $70\ \mu\text{m}$ propagation length.

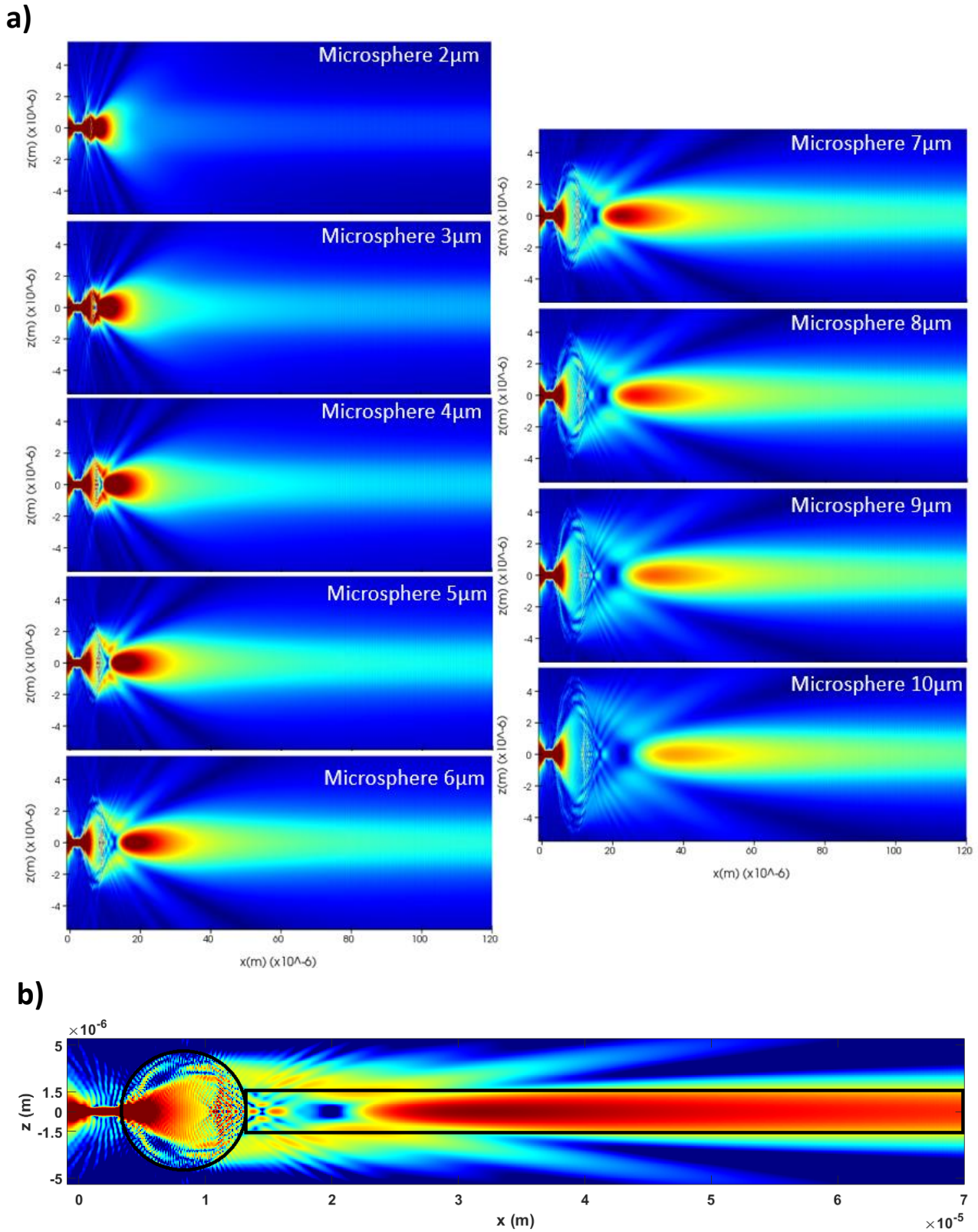


Figure S5. Coupling for a microsphere with $n=2.0$. a) Representative propagation simulations, over $120 \mu\text{m}$ length, for specific diameters and distance $L=0\mu\text{m}$. b) Coupling mechanism for the optimum case with maximum coupling with diameter $9 \mu\text{m}$ and $L=0\mu\text{m}$ over $70 \mu\text{m}$ propagation length.

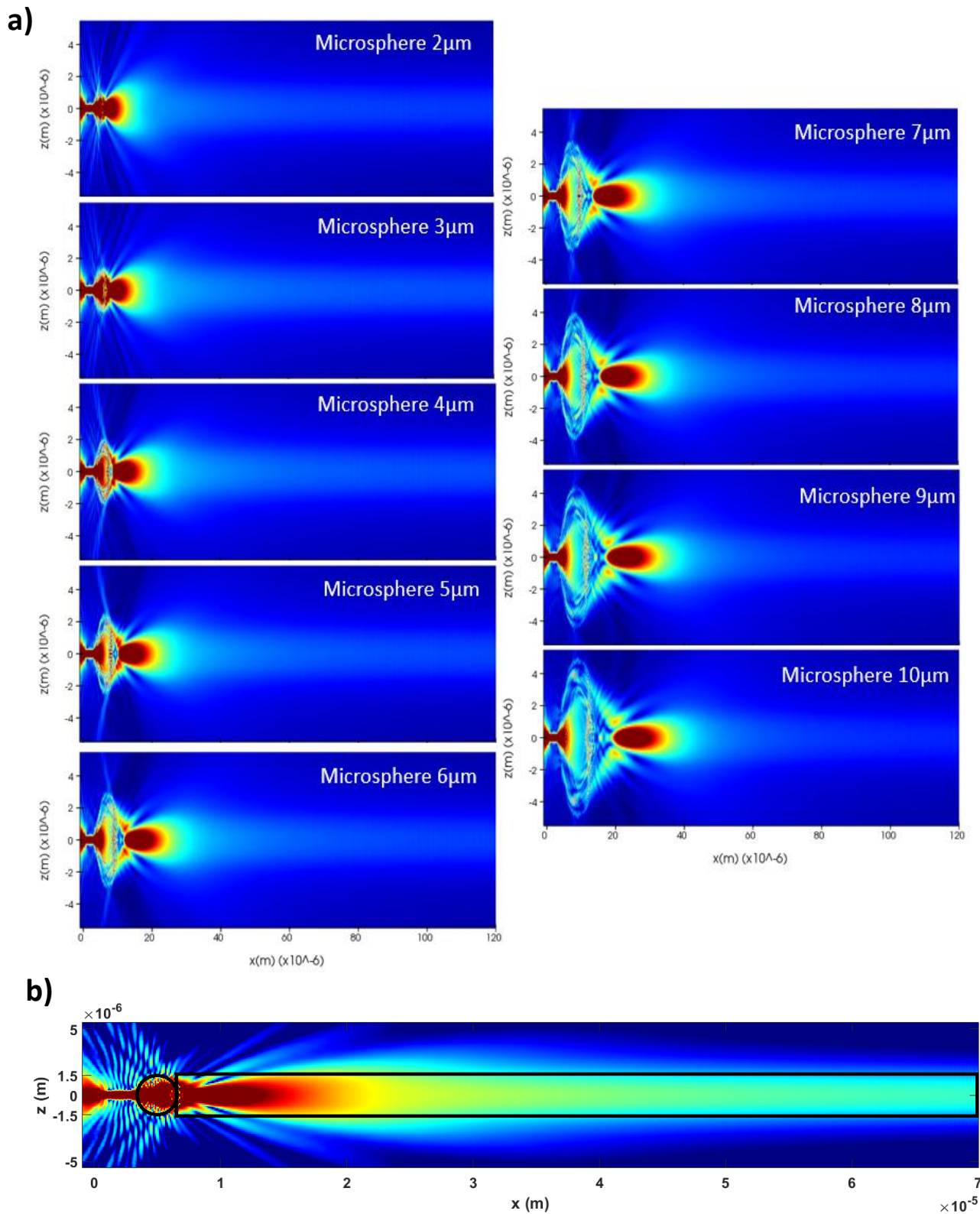


Figure S6. Coupling for a microsphere with $n=2.2$. a) Representative propagation simulations, over 120 μm length, for specific diameters and distance $L=0\mu\text{m}$. b) Coupling mechanism for the optimum case with maximum coupling with diameter 3 μm and $L=0\mu\text{m}$ over 70 μm propagation length.

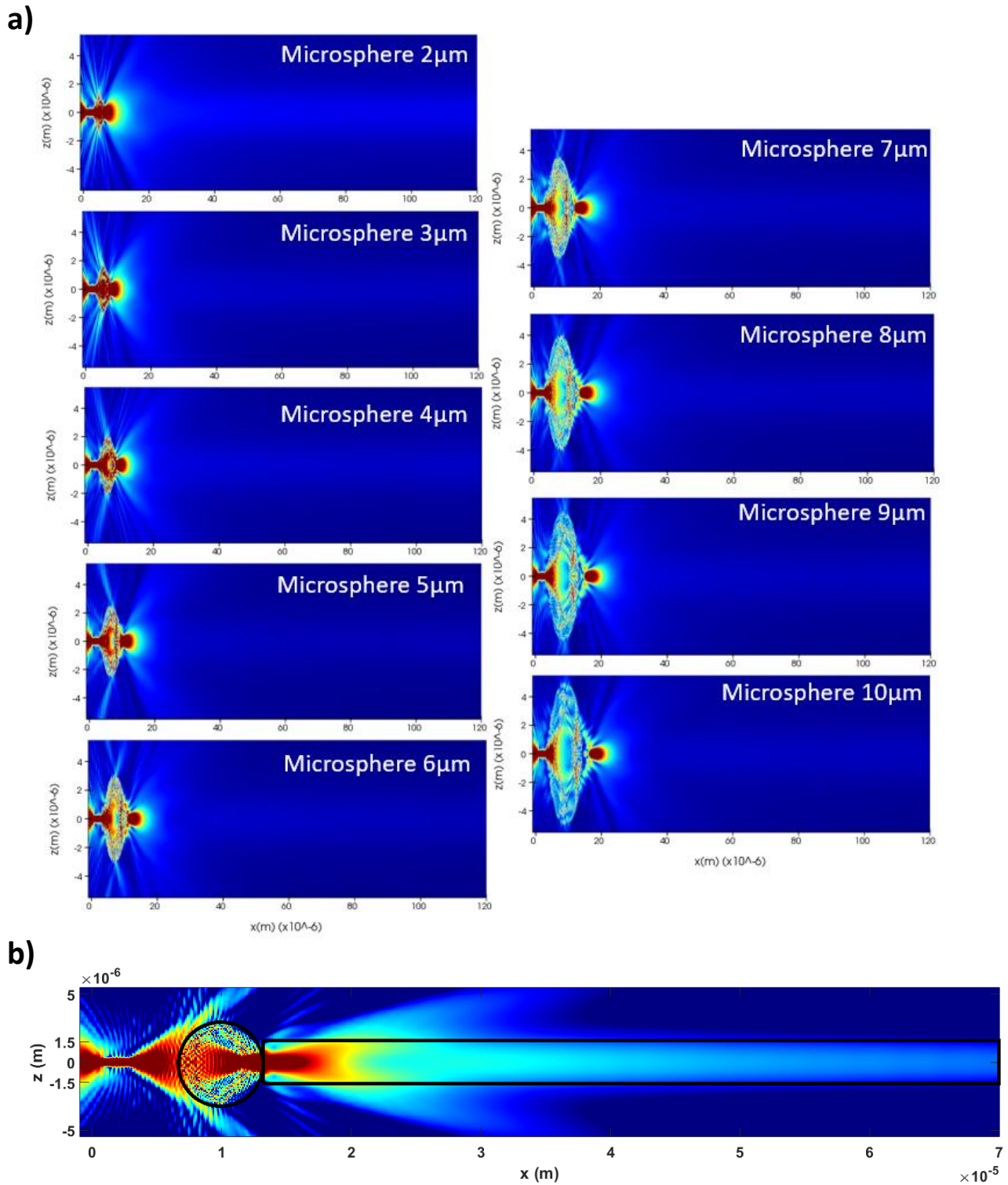


Figure S7. Coupling for a microsphere with $n=2.5$. a) Representative propagation simulations, over $120\ \mu\text{m}$ length, for specific diameters and distance $L=3\ \mu\text{m}$. b) Coupling mechanism for the optimum case with maximum coupling with diameter $6\ \mu\text{m}$ and $L=3\ \mu\text{m}$ over $70\ \mu\text{m}$ propagation length.